2

X-672-72-259
PREPRINT

NASA TM X- 65967

# LOW INTENSITY BALMER EMISSIONS FROM THE INTERSTELLAR MEDIUM AND GEOCORONA



R. J. REYNOLDS
F. L. ROESLER
F. SCHERB

JUNE 1972



GSFC
GODDARD SPACE FLIGHT CENTER
GREENBELT, MARYLAND

# LOW INTENSITY BALMER EMISSIONS FRO.: THE INTERSTELLAR MEDIUM AND GEOCORONA

R. J. Reynolds*
NASA, Goddard Space Flight Center
Greenbelt, Maryland

and

F. L. Roesler and F. Scherb
Physics Department, Univserity of Wisconsin
Madison, Wisconsin

Received: ________________

*National Academy of Sciences Resident Research Associate

# LOW INTENSITY BALMER EMISSIONS FROM THE INTERSTELLAR MEDIUM AND GEOCORONA

## ABSTRACT

Galactic and non-galactic components of the diffuse $H\alpha$ and $H\beta$ night sky emissions have been resolved with a Fabry-Perot spectrometer. The non-galactic component of both lines accounts for most of the emission at galactic latitudes greater than $30^{\circ}$. The intensities of the galactic component yield values for the average ionization rate per hydrogen atom that are between $10^{-15}$ and $10^{-14} s^{-1}$ assuming steady-state ionization.

## I. INTRODUCTION

A study of faint, diffuse galactic $H\alpha$ and $H\beta$ emissions has been started using a 150 mm diameter pressure-scanned Fabry-Perot spectrometer at the coude' focus of the 36-inch telescope at Goddard Space Flight Center in Maryland. The spectrometer has a spectral resolving power of 25,000 (12 $kms^{-1}$) and a circular 6.5' field of view. Faint $H\beta$ emissions that do not appear to be associated with any known HII regions have previously been observed by

Johnson (1971) using interference filters and by Daehler et al. (1968) and Reay and Ring (1969) using Fabry-Perot spectrometers, but low spectral resolution prevented them from using radial velocity shifts to discriminate between galactic and possible local emission sources. Since the galactic hydrogen often has radial velocities of $\pm$ 25km $s^{-1}$ or more with respect to the earth, it has been possible with the present spectrometer's 12 km $s^{-1}$ resolution to resolve the unshifted (probably geocoronal) $H\alpha$ and $H\beta$ lines from the galactic lines, and thus unambiguously determine for a variety of observation directions the relative contributions of each source to the line intensites.

## II. OBSERVATIONS

Figure 1 shows two $H\beta$ scans in a direction of low galactic latitude ($l^{II} = 184.5^o$, $b^{II} = -5.8^o$) at two different times of the year. The photomultiplier count rates are plotted as a function of the radial velocity with respect to the earth. In figure 1a the galactic local standard of rest (LSR) velocity was at -11 km $s^{-1}$ and there appeared to be a single $H\beta$ line. Three months later (figure 1b) the LSR velocity had shifted to +30km $s^{-1}$ with respect to the earth and there appeared two clearly resolved lines -- a galactic $H\beta$ line near the LSR velocity and a fainter, narrower $H\beta$ line at 0 km $s^{-1}$. Scans of the $H\alpha$ lines in this direction are shown in figure 2. The galactic $H\alpha$ line at +35 km $s^{-1}$ in these two scans is unfortunately nearly obscured by and OH airglow line leaking through a side transmission peak of the Fabry-Perot etalon. This difficulty has subsequently been eliminated by adding a second etalon to the system.

Using the absolute H$\alpha$ and H$\beta$ intensity measurements of HII regions (Ishida and Kawajii 1968; Boyce 1966; O'Dell, et al. 1967; Schmitter 1971) and planetary nebulae (Collins, et al. 1960), the non-galactic and galactic H$\beta$ emission lines in figure 1b were found to have intensities of 0.3-0.4 R and 0.6-0.8 R respectively. ($1R = 8 \times 10^4$ photons $cm^{-2}$ $s^{-1}$ sterad$^{-1}$.) The unshifted H$\alpha$ lines in figure 2a and 2b have intensities of 1.5-2.0R and 3.2-4.5 R respectively. The line widths imply temperatures lower than 1500$^{o}$K for the non-galactic source and 5500 $\pm$ 1500$^{o}$K for the galactic source assuming that the widths are due to thermal motions only.

a) Non-Galactic Balmer Emissions

Observations have been made in more than 40 directions between 1971 October and 1972 March. The non-galactic H$\alpha$ and H$\beta$ lines are centered (to within a 2 km $s^{-1}$ measurement accuracy) on 0 km $s^{-1}$, and both have line widths implying a temperature lower than 1500$^{o}$K for the emitting region.

Figure 3 demonstrates how the observed intensities of these lines varied with changing geometry between the observation direction and the sun. The count rates above background at the peak of the line are plotted as a function of the angle $\theta$ between the observation direction and the direction to the sun. The H$\alpha$ and H$\beta$ count rates obtained on various dates between January and March 1972 in a single low galactic latitude direction ($l^{II} = 184.5^{o}$, $b^{II} = -5.8^{o}$) are plotted together with the H$\beta$ rates observed in a variety of directions (and solar depression angles) during a single night on 1971 November 21-22. The rates have been normalized for equal atmospheric transmission. The data in figure 3 indicate that;(1) the H$\beta$ intensity has remained virtually constant between 1971 November and 1972 March for $\theta \geq 90^{o}$; (2) although the H$\alpha$ intensity does vary significantly with changing geometry as has been observed before by others and is easily expalined by the scattering L$\beta$ in the geocorona, the H$\beta$ intensity for $\theta \geq 90^{o}$ appears to be quite independent of $\theta$, as well as solar depression angle as is seen from the lack of signigicant scatter of the points about the dashed line. This result is difficult to explain by scattering of solar L$\gamma$ in the geocorona, since in such a case the H$\beta$ intensity should continue to decrease with increasing $\theta$ beyond $90^{o}$ because fewer L$\gamma$ photons can be scattered into these directions. Reay and Ring (1969) observed similar behavior for H$\beta$ emission at high galactic latitudes using a Fabry-Perot spectrometer with relatively low (36 km $S^{-1}$) resolution. However, even though they were not able to spectrally eliminate possible galactic contributions, their quoted absolute intensities are a factor of 3 or 4 times lower than those presented here. This discrepancy may be evidence of significant changes in the intensity of the $H\beta$ line over a period of years.

Both the narrow line width and the 0 km $s^{-1}$ radial velocity eliminate the possibility that this emission is due to either interplanetary hydrogen or tropspheric scattering of bright astronomical sources (Tinsley 1970). Also neither line was present in the spectrum of scattered terrestrial lights. Therefore, the origin of both lines $H\beta$ as well as $H\alpha$, is probably the geocorona. The uniform, bright 0.5 R $H\beta$ flux for $\theta \geq 90^{o}$ as well as the low absolute $H\alpha$:$H\beta$ ratio of 4-5:1 for the $\theta = 143^{o}$ observation suggest then that perhaps there is a second Balmer line producing mechanism is the geocorona (Kondo and Kupperian 1967) in addition to the excitation of hydrogen by direct and scattered solar Lyman radiation. More careful measurements of the position of these lines may help determine the mechanism of excitation. Balmer lines which are produced by absorption of Lyman radiation involve only the transitions $n^2P - 2^2S$. Such lines will have and apparent blue shift of approximately 2 km $s^{-1}$ with respect to lines produced as a result of recombination radiation which include additional fine structure transitions.

b) Galactic Balmer Emissions

From observations convering galactic latitudes $-60^{\circ}$ to $+87^{\circ}$ and galactic longitudes $60^{\circ}$ to $250^{\circ}$, it appears that, with a few possible exceptions, e.g., high galactic latitude HII regions(Lynds 1965) and radio spurs(Meaburn 1967), the unshifted (geocoronal) lines account for nearly all the $H\alpha$ and $H\beta$ emissions from directions more than $30^{\circ}$ from the galactic plane. An $H\beta$ scan at $+23^{\circ}$ galactic latitude and an $H\alpha$ scan near the galactic pole, shown in figures 4a and 4b respectively, are typical of data from high galactic latitudes. The excess emission on the blue side of the unshifted $H\beta$ line in figure 4a indicates the presence of galactic $H\beta$ emission (0.3-0.7 R) from this direction. No such asymmetry is apparent in the $H\alpha$ line in figure 4b. Assuming that the emission line would be at nearly the same radial velocity as the neutral hydrogen, this lack of asymmetry then implies a galactic $H\alpha$ intensity $I\alpha < 0.4R$ in the galactic pole direction. Since the galactic hydrogen rarely has a radial velocity more than about $\pm$ 40 $kms^{-1}$ with respect to the laboratory velocity, the study of the galactic Balmer emissions at high galactic latitudes will often be limited to observations of asymmetries in the wings of the unshifted geocoronal lines.

## III. THE INTERSTELLAR MEDIUM

Observations of diffuse galactic Balmer lines can be used to determine various properties of the interstellar medium. In directions of low visual extinction, e.g., high galactic latitudes, or where the extinction as a function of distance is well known, the intensity $I\beta$ of the galactic H$\beta$ emission can be used (assuming steady-state) to determine the average ionization rate per hydrogen atom $\langle\zeta_H\rangle$ along the line of sight. When the extinction is negligible $\langle\zeta_H\rangle$ is given by the relation (Reynolds et al. 1971)

$$\langle\zeta_H\rangle = 105\ I\beta/N_H \quad , \tag{1}$$

where $N_H$ is the columnar atomic hydrogen density in units of $cm^{-2}$ and $I\beta$ is in units of photons $cm^{-2}s^{-1}sterad^{-1}$. Using values for the emissivity of hydrogen given by Pengelly (1964), the emission measure e.m., can also be computed from $I\beta$ and an estimate of the temperature, which can be obtained from the line width, when observable, and assumed contributions of turbulence. (Upper limits to the temperature and thus the emission measure can always be obtained from the line width by assuming thermal broadening only.) When the observations are made in directions near pulsars, the pulsar dispersion measure d.m. can be combined with e.m. (or only an upper limit on e.m.) to set both a lower limit on the total distance L along the line of sight occupied by the ionized hydrogen, given by (Reynolds et al. 1971)

$$L \geq (d.m.)^2 /e.m., \tag{2}$$

and an upper limit on the average electron density $<n_e>$ within the regions of ionization, given by (Reynolds et al. 1971).

$$<n_e> \leq e.m./d.m. \tag{3}$$

Table 1 summarizes the results of applying this analysis to the three observation directions discussed above. For the low-galactic-latitude direction which is near the Crab Nebula pulsar, two separate cases were considered. In column (a) the emission was assumed to be originating from a single localized region well within one Hβ mean free path length (1 kpc) of the sun so that turbulent velocities and extinction could be neglected. However, the resulting large lower limit on L suggests that the region may not be localized. Therefore, in column (b) the emission was assumed to be originating from a large number of regions distributed uniformly along the total line of sight distance through the galactic disk. The random velocity distribution of these regions was assumed to have a FWHM of 7 km s$^{-1}$ -- a value derived from the random motions of the HI clouds since broadening due to galactic rotation is negligible in this near anti-center direction. It should be noted that even if non-thermal velocity contributions to the observed line width were greater than 7 km $s^{-1}$ resulting in a lower temperature and lower emission measure for the emitting region, the value of $\langle \zeta_H \rangle$ would remain unchanged and the limits on $\langle n_e \rangle$ and L would become even more stringent, i.e., the upper limit on $\langle n_e \rangle$ would decrease and the lower limit on L would increase. Corrections for extinction were made using data given by O'Dell (1962) for this direction. Since there are two pulsars near this direction -- the Crab pulsar NP 0532 (9' West) with d.m. = 57 $cm^{-3}$pc and NP 0527 (1.5$^{o}$ West) with d.m. = 51 $cm^{-3}$pc -- an average dispersion measure of 54 $cm^{-3}$pc was chosen for the computations.

Columns (c) and (d) of Table 1 summarize the observational data in the two higher galactic latitude directions. Since no line profiles were obtained in these directions, in order to compute e.m. the temperature was assumed to be approximately the same (5000$^{o}$K) as in the low latitude direction. But as mentioned above, the limits on $\langle n_e \rangle$ and L and values of $\langle \zeta_H \rangle$ continue to hold for any temperature less than 5000$^{o}$K. Note also that even though no galactic emission was detected from the galactic pole direction, the value of the pulsar dispersion measure and the upper limit on $I\alpha$ still allow limits to be placed on e.m., $<n_e>$, L, and $<\zeta_H>$ in this direction.

The data in Table 1 indicate that in the two directions near pulsars where limits could be placed on L and $<n_e>$, the regions of ionization occupy a considerable fraction of the line of sight distance through the galactic disk with $<n_e> \leq 0.2$ cm$^{-3}$. A value of $<\zeta_H>$ of about 3 x $10^{-15}$s$^{-1}$ H-atom$^{-1}$ is consistent with the data in all three directions. However, in other directions (to be discussed below) where the diffuse galactic emission is brighter, values for $<\zeta_H>$ are as high as 20-30 x $10^{-15}$ s$^{-1}$ H-atom$^{-1}$.

With the limited number of observations, the large scale structure of the galactic Balmer emission is not yet clear. The only region of the galactic plane that has been studied in any detail is the region near the galactic anticenter ($160^o < l^{II} < 200^o$ and $-20^o < b^{II} < +10^o$). Figure 5 is a map of this region in galactic coordinates denoting the observation directions (open circles) and the brightness contours (solid lines) around the brighter regions of the diffuse galactic $H_\beta$ emission. In the directions outside the contour lines, faint galactic emission appears to be present with intensities of approximately 0.3R to 1.0R. The large "bright" region emphasized by the contour lines could be an extension of the HII region surrounding $\lambda$Orionis

(Sharpless and Osterbrock 1952) or part of a very large region of ionization surrounding the entire Orion association (outlined by a dashed oval). Another large region of ionization appears to be present in the Cygnus region of the galactic plane between galactic longitudes $70^{o}$ and $100^{o}$. This region has also been observed by Montbriand, et al. (1965) and Courtes and Sivan (1972) using photographic methods. It is important to determine whether these regions are isolated anomalies superimposed upon a fainter, more uniform emission whose intensity is strongly correlated with $N_H$ (in directions of low extinction), or whether all the diffuse Balmer emission is the result of a superposition of many of these regions filling the galactic disk. The former case would suggest a steady-state ionization process involving cosmic rays, x-rays, or UV photons (Hawakawa et al. 1961; Silk and Werner 1970; Walmsley and Grewing 1971), while the latter case would suggest possible non-steady-state processes (Bottcher et al. 1970).

In an effort to resolve these questions, a more extensive survey is planned, and additional interstellar emission lines will be studied including the [OIII] 5007Å line and lines of HeI.

We are grateful to Mr. John Trauger for his work on the optical coatings and to Dr. E. Boldt for helpful disucssions. This work has been supported in part by the National Academy of Sciences through a resident research associateship, by the National Aeronautics and Space Administration through grant NGL 50-002-162, by the Atmospheric Sciences Section, National Science Foundation through grant GA-15733, and by the University of Wisconsin Graduate School through funds provided by the Wisconsin Alumni Research Foundation.

TABLE 1

PROPERTIES OF THE INTERSTELLAR MEDIUM
IN THREE SELECTED DIRECTIONS

| Parameters | a | b | c | d |
|---|---|---|---|---|
| | $b = -5.8^{\circ}$ $l = 184.5^{\circ}$ | | $b = +23^{\circ}$ $l = 178^{\circ}$ | $b = +86.5^{\circ}$ $l = 253^{\circ}$ |
| | NP 0532 and NP 0527 | | - | PSR 1237 |
| d.m. ($cm^{-3}$pc) ......... | 54. | 54. | - | 8.5 |
| $N_H$ ($X10^{-20}cm^{-2}$) ....... | 44. | 44. | 7. | 2.3* |
| T($^{\circ}$K) .................. | 5500 ± 1500 | 4000 ± 1500 | 5000† | 5000† |
| Iβ (R) (galactic) ..... | 0.7 ± 0.2 | 0.7 ± 0.2 | 0.4 ± 0.2 | - |
| Iα (R) (galactic) ..... | - | - | - | <0.4 |
| e.m. ($cm^{-6}$pc) ......... | 4. ± 1. | 8. ± 2. | 2. ± 1. | <0.6 |
| $<n_e>$ ($cm^{-3}$) ........... | ≤0.07 ± 0.02 | ≤0.2 ± 0.1 | - | <0.1 |
| L (pc) ................ | ≥700 ± 200 | ≥400 ± 100 | - | >100 |
| $<\zeta_H>$($X10^{15}s^{-1}$ H-atom$^{-1}$) | - | 3. ± 1. | 4. ± 2. | <4. |

* interpolated from measurements 4° away

† assumed (not measured)

## REFERENCES


Bottcher, C., McCray, R. A., Jura, M., and Dalgarno, A. 1970, Ap. Letters, 6, 237.

Boyce, B. 1966, Lowell Observatory Bull. No. 130, 215.

Collins II, G. W., Daub, C. T., and O'Dell, C. R. 1960, Ap. J., 133, 471.

Courtes, G. and Sivan, J. P. 1972, preprint.

Daehler, M., Mack, J. E., Stoner, Jr., J. O., Clark, D., and Ring, J. 1968, Planet. Space Sci., 16, 795.

Hayakawa, S., Nishimura, S., and Takeyanagi, K. 1961, Publ. Astr. Soc. Japan, 13, 184.

Ishida, K., and Kawajiri, N. 1968, Publ. Astr. Soc. Japan, 20, 95.

Johnson, H. M. 1971, Ap. J. 164, 379.

Kondo, Y. and Kupperian, Jr., J. E. 1967, J. Geophys. Res., 72, 6091.

Lynds, B. T. 1965, Ap. J. Suppl., 4, 257.

Meaburn, J. 1967, Z. Astrophys. 65, 93.

Montbriand, L. E. J., Tinsley, B. A., and Jones, V. A. 1965, Can. J. Phys., 43, 782.

O'Dell, C. R. 1962, Ap. J., 136, 809.

O'Dell, C. R., York, G., and Henize, G. 1967, Ap. J. 150, 835.

Pengelly, R. M. 1964, M.N.R.A.S., 127, 145.

Reay, N. K. and Ring, J. 1969, Planet. Space Sci., 17, 561.

Reynolds, R. J., Roesler, F. L., Scherb, F., and Boldt, E. 1971, The Gum Nebula and Related Problems (Proceedings of a Conference at Goddard Space Flight Center, Preliminary Edition), pp. 182-209.

Schmitter, E. F. 1971, A. J., 76, 571.

Sharpless, S. and Osterbrock, D. 1952, Ap. J. 115, 89.

Silk, J. and Werner, M. W. 1969, Ap. J. 158, 185.

Tinsley, B. A. 1970, Space Res., 10, 582.

Walmsley, M. and Grewing, M. 1971, Ap. Letters, 9, 185.

FIGURE CAPTIONS

Figure 1. H-beta scans in the direction: $l^{II} = 184.5^{o}$, $b^{II} = -5.8^{o}$. (a) Sum of scans on 1971 October 14-15 and 1971 October 26-27. (b) Sum of scans on 1972 January 19-20. The LSR and the position and FWHM of the neutral galactic hydrogen as measured by 21-cm radiation are also indicated.

Figure 2. H-alpha scans in the direction: $l^{II} = 184.5^{o}$, $b^{II} = -5.8^{o}$. (a) Sum of scans on 1972 January 19-20. (b) Single scan on 1972 February 14-15. The peaks of the galactic Hα lines, nearly obscured by an OH airglow line, are denoted by dashed curves.

Figure 3. Non-galactic emission. The Hα and Hβ count rates above background at the line center vs. the angle θ between the observation direction and the sun. A rate of 1 $s^{-1}$ corresponds to an intensity of approximately 0.5R for Hβ and 1.0R for Hα.

Figure 4. (a) Sum of Hβ scans in the direction: $l^{II} = 170^{o}$, $b^{II} = +23^{o}$. (b) An H-alpha scan in the direction: $l^{II} = 253^{o}$, $b^{II} = +86.5^{o}$. The LSR and the position and FWHM of the neutral galactic hydrogen as measured by 21-cm radiation are indicated.

Figure 5. Galactic anticenter region. Open circles, observation direction; crosses, positions of bright stars in the Orion constellation and Pleiades cluster; cross-hatched regions, bright HII regions; solid lines, brightness contours around the brighter regions of diffuse galactic emission. Contour values are counts per second above background at line center. A rate of $1 s^{-1}$ corresponds to an intensity of approximately 0.8R $H\beta$.



NASA-GSFC COML., Arlington, Va.

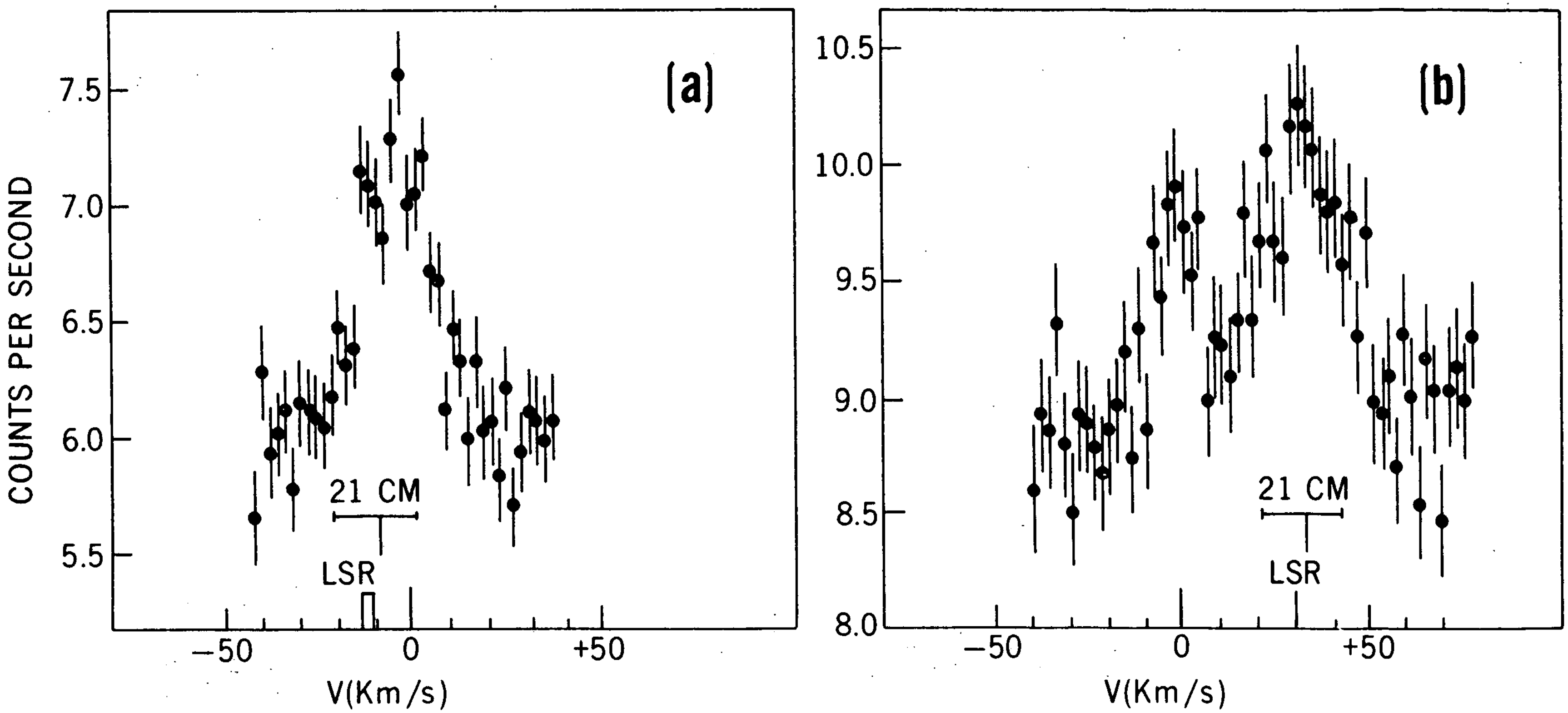

COUNTS PER SECOND
7.5
7.0
6.5
6.0
5.5
(a)
21 CM
LSR
−50
0
+50
V(Km/s)
10.5
10.0
9.5
9.0
8.5
8.0
(b)
21 CM
LSR
−50
0
+50
V(Km/s)

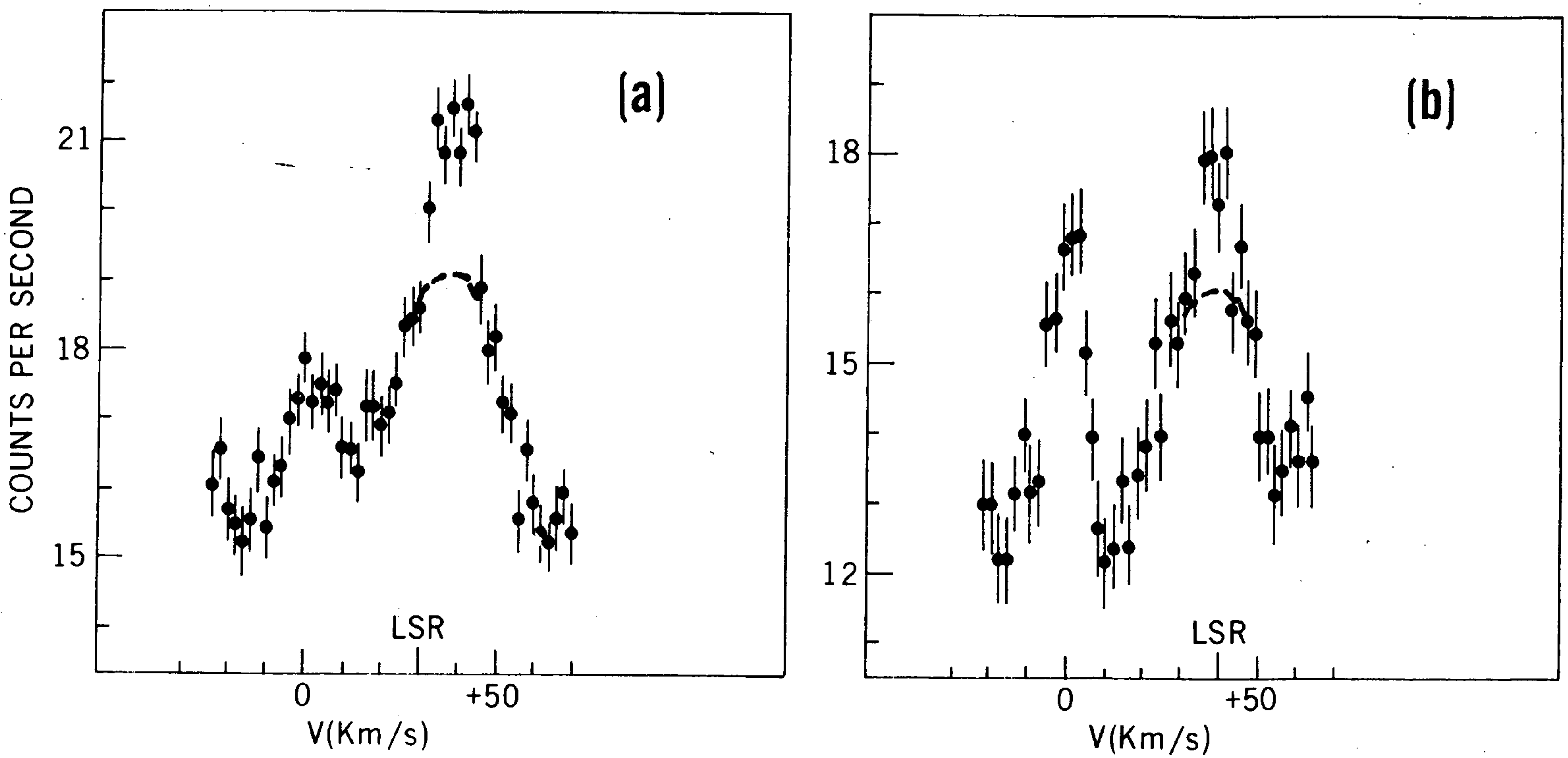

COUNTS PER SECOND
15
18
21
(a)
LSR
0
+50
V(Km/s)
12
15
18
(b)
LSR
0
+50
V(Km/s)

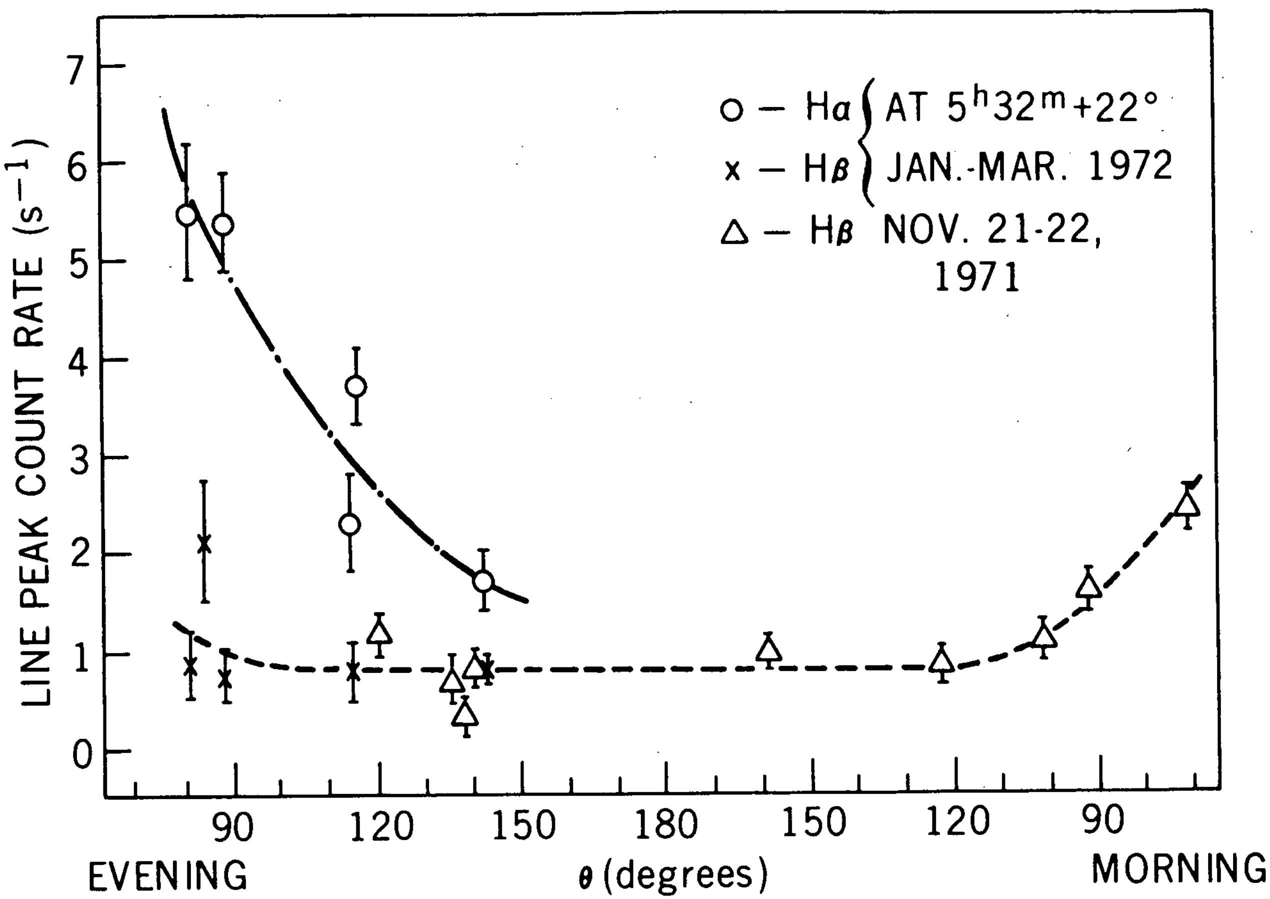

LINE PEAK COUNT RATE ($s^{-1}$)
0
1
2
3
4
5
6
7
○ – Hα
x – Hβ
AT $5^h32^m + 22°$
JAN.-MAR. 1972
△ – Hβ NOV. 21-22, 1971
90
120
150
180
150
120
90
EVENING
θ (degrees)
MORNING

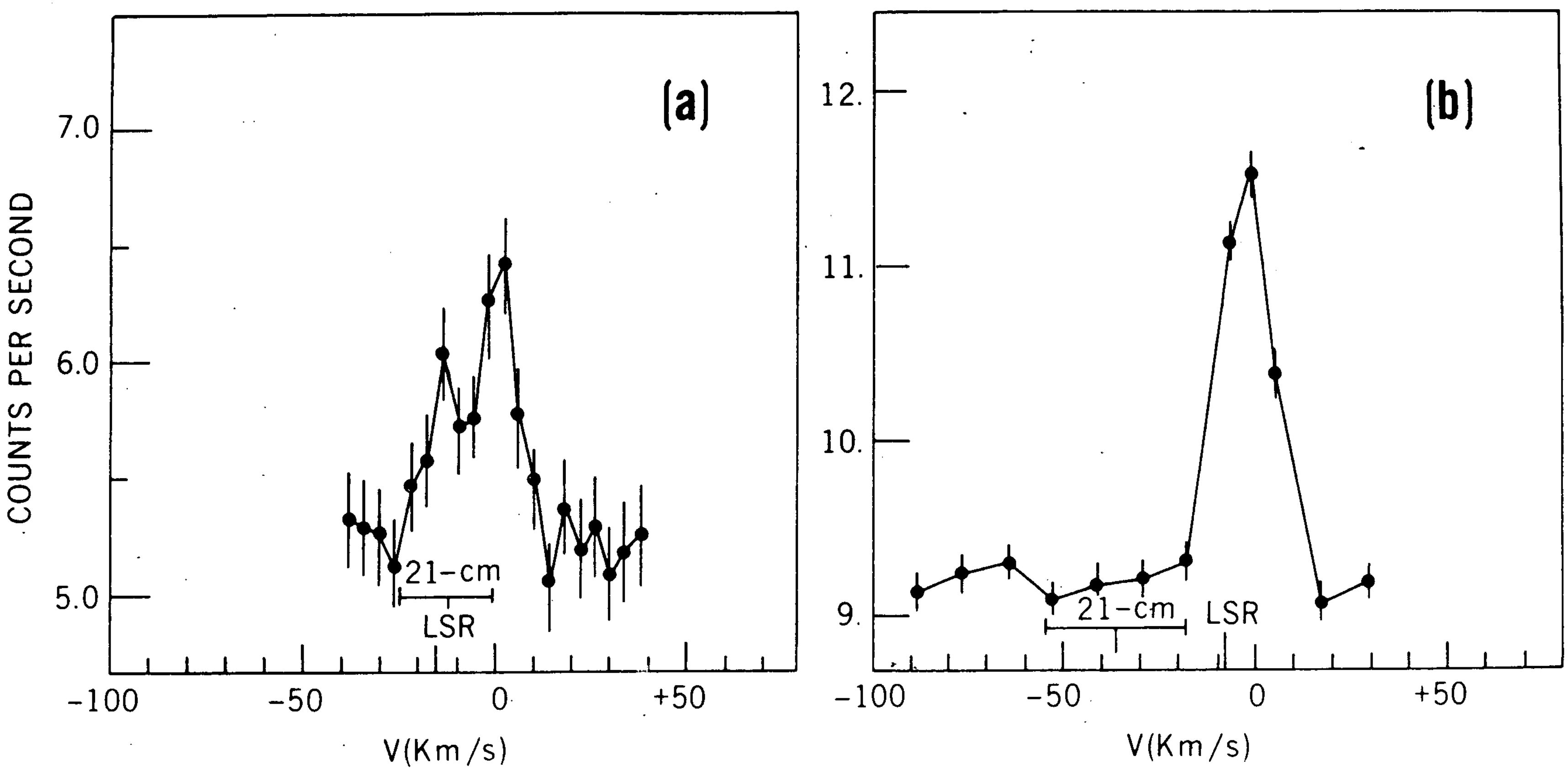

(a)
(b)
COUNTS PER SECOND
7.0
6.0
5.0
12.
11.
10.
9.
21-cm
LSR
21-cm
LSR
-100
-50
0
+50
-100
-50
0
+50
V(Km/s)
V(Km/s)

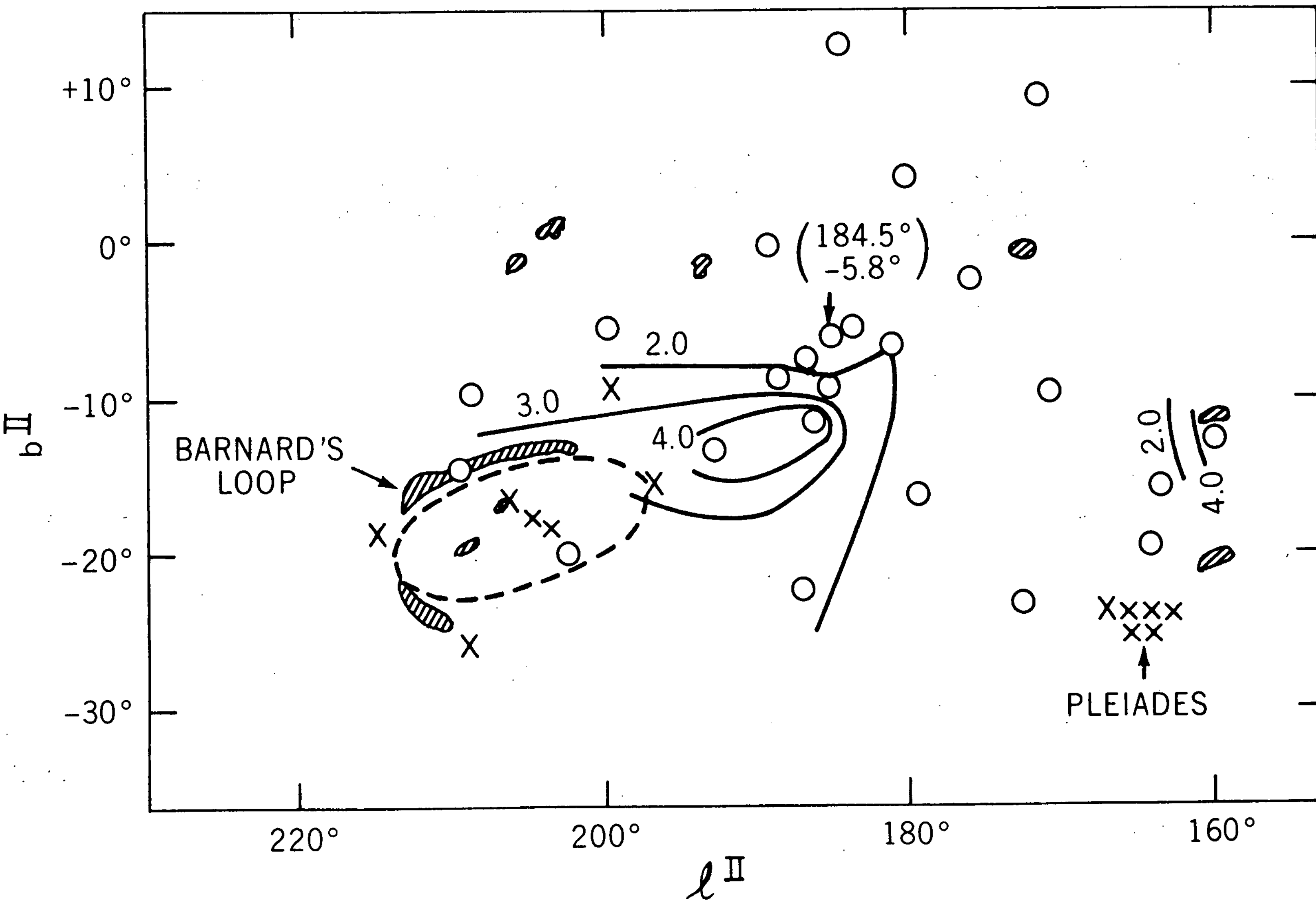

+10°
0°
−10°
−20°
−30°
$b^{II}$
220°
200°
180°
160°
$\ell^{II}$
(184.5°
−5.8°)
2.0
3.0
4.0
BARNARD'S
LOOP
2.0
4.0
PLEIADES